# APP/APLP2 expression is required to initiate endosome-nucleus-autophagosome trafficking of glypican-1-derived heparan sulfate.

Cheng, Fang; Cappai, Roberto; Lidfeldt, Jon; Belting, Mattias; Fransson, Lars-Åke; Mani, Katrin

*Published in:*
Journal of Biological Chemistry

*DOI:*
10.1074/jbc.M114.552810

2014

# APP/APLP2 expression is required to initiate endosome-nucleus-autophagosome trafficking of glypican-1-derived heparan sulfate*


**Fang Cheng[1], Roberto Cappai[2], Jon Lidfeldt [3], Mattias Belting[3, 4], Lars-Åke Fransson[1] and Katrin Mani[1, 5]**

From the [1]Department of Experimental Medical Science, Division of Neuroscience, Glycobiology Group, Lund University, Biomedical Center A13, SE-221 84, Lund, Sweden, the [2]Department of Pathology, Bio21 Molecular Science and Biotechnology Institute, The University of Melbourne, VIC 3010, Australia and,[3]Department of Clinical Sciences, Section of Oncology and Pathology, Lund University, SE-221 85, Lund, Sweden, [4]Skåne Oncology Clinic, Lund Sweden.

[5]To whom correspondence should be addressed: Katrin Mani, Department of Experimental Medical Science, Division of Neuroscience, Glycobiology Group, Lund University, Biomedical Center A13, SE-221 84, Lund, Sweden, Tel: ++46 46 222 4044, E-mail: katrin.mani@med.lu.se


*Running title:* APP supports nuclear targeting of heparan sulfate


*Keywords:* Amyloid precursor protein; Amyloid beta; Autophagy; Endosomes; Glypican-1; Heparan sulfate; Nuclear translocation


---


**Background:** The normal function of the amyloid precursor protein of Alzheimer´s disease is poorly understood.

**Results:** Amyloid precursor protein controls nuclear translocation of heparan sulfate released from its parent proteoglycan in endosomes.

**Conclusion:** An endosome-cytosol-nucleus-autophagosome traffic route for heparan sulfate is demonstrated.

**Significance:** Provides a basis for better understanding of the pathogenesis of the major form (sporadic) of Alzheimer´s disease.

**ABSTRACT**

**Anhydromannose (anMan)-containing heparan sulfate (HS) derived from the proteoglycan glypican-1 (Gpc-1) is generated in endosomes by an endogenously or ascorbate induced SNO-catalyzed reaction. Processing of the amyloid precursor protein**

**(APP) and APP-like protein 2 (APLP2) by β- and γ-secretases into amyloid beta (Aβ) and Aβ-like peptides also takes place in these compartments. Moreover, anMan-containing HS suppresses the formation of toxic Aβ assemblies *in vitro*. We show by using deconvolution immunofluorescence microscopy with an anMan-specific monoclonal antibody as well as $^{35}$S-labeling experiments that expression of APP/APLP2 is required for ascorbate-induced transport of HS from endosomes to the nucleus. Nuclear translocation was observed in wild-type mouse embryonic fibroblasts (Wt-MEF), Tg2576 MEF and N2a neuroblastoma cells but not in APP$^{-/-}$ and APLP2$^{-/-}$ MEF. Transfection of APP$^{-/-}$ cells with a vector encoding APP restored nuclear import of anMan-containing HS. In Wt-MEF and N2a neuroblastoma cells exposed to β- or γ-secretase inhibitors, nuclear translocation was greatly impeded, suggesting involvement of APP/APLP2 degradation products. In Tg2576 MEF, the β-inhibitor blocked transport but the γ-inhibitor did not. During chase in ascorbate-free medium, anMan-containing HS disappeared from the nuclei of Wt-MEF.**

**Confocal immunofluorescence microscopy showed that they appeared in acidic, LC3-positive vesicles in keeping with an autophagosomal location. There was increased accumulation of anMan-containing HS in nuclei and cytosolic vesicles upon treatment with chloroquine indicating that HS was degraded in lysosomes. Manipulations of APP expression and processing may have deleterious effects upon HS function in the nucleus.**

---

Biochemical and genetic evidence points to a central role for the amyloid precursor protein (APP)[4] in Alzheimer´s disease (AD) pathogenesis. APP and its paralogs, amyloid precursor-like protein 1 and 2 (APLP1 and APLP2) are proteolytically processed by α-, β- and γ-secretases to large soluble N-terminal ectodomains, small soluble internally derived peptides and C-terminal membrane-bound domains. The intracellularly released amyloid beta peptides (mostly Aβ40 and Aβ42) derived from APP by combined β- and γ-cleavage can aggregate into neurotoxic oligomers and insoluble fibrils that accumulate in AD plaques (1-5). Secreted Aβ peptides have a regulatory role in transmitter release at hippocampal synapses under physiological conditions (6). However, the intracellular function of APP, APLP1, APLP2 and their degradation products remains largely unknown (7).

APP and Aβ peptides bind strongly to the heparan sulfate (HS) proteoglycan glypican-1 (Gpc-1) *in vitro* and APP and Gpc-1 are colocalized inside cells (8-10). Gpc-1 can be internalized via a caveolin-1 associated pathway and is recycled via endosomes and the Golgi. During or after uptake, specific cysteines in the Gpc-1 core protein are S-nitrosylated (SNO) in a reaction that is dependent on copper that could be provided by APP. In endosomes, the Gpc-1 HS chains are deaminatively cleaved in an SNO-catalyzed reaction resulting in release of HS chains and oligosaccharides containing reducing terminal anhydromannose (anMan). This reaction can also be induced by exogenously supplied ascorbate (11-17). There appears to be a functional relationship *in vivo* between the HS- and copper-binding activities of APP/APLP2 and their modulation of Gpc-1 autoprocessing in neurons (10).

HS as well as other glycosaminoglycans have been found in various cell nuclei (18-21). Moreover, xyloside-primed HS is secreted and re-internalized by T24 bladder carcinoma cells and processed to anMan-positive degradation products that are targeted to the nucleus (22). Whether and how HS degradation products penetrate the endosomal membrane to reach the cytosol and then the nucleus has remained unsolved (23).

We have previously shown that anMan immunoreactivity is present in AD plaques, and that a 50-55-kDa anMan- and Aβ-immunoreactive component can be isolated from fibroblasts of AD mice (Tg2576), and that anMan-containing HS degradation products can suppress Aβ42 oligomerization *in vitro* (24). More recently we have shown that non-toxic Aβ peptide assemblies are formed when oligomerization/aggregation takes place while anMan-containing HS is simultaneously generated from Gpc-1-SNO (25). As this may reflect normal functions for APP, Aβ peptides and anMan-containing HS we decided to examine whether APP and its degradation products play a role in the generation and/or localization of anMan-containing HS. We show by using wild-type, $APP^{-/-}$, $APLP2^{-/-}$ and Tg2576 mouse embryonic fibroblasts (MEF) and mouse N2a neuroblastoma cells that APP/APLP2 expression is required to initiate transport of anMan-containing HS from endosomes via the cytosol into the nucleus. HS then returns to the cytosol and accumulates in autophagosomes.

## EXPERIMENTAL PROCEDURES

*Materials*- Mammalian transfection plasmid pIRESpuro-APP695 (Clontech laboratories, Inc. Mountain View, CA, USA) encoded the APP695 cDNA. Mouse embryonic fibroblasts (MEF) from wild-type (Wt), $APP^{-/-}$, $APLP2^{-/-}$, and Tg2576 mice as well as mouse N2a neuroblastoma cells were grown as described earlier (10, 14, 24). A polyclonal antibody (pAb) to LC3 (L8918) and chloroquine were obtained from Sigma. The β-secretase inhibitor LY2811376 and the γ-secretase inhibitor BMS-708163 (Avagacestat) were both purchased from Selleckchem. pAbs to the C-terminal of APP (A8717), a mAb recognizing anMan-containing HS (12), various secondary antibodies, heparinase I and III, the DNA staining compound 4,6-diamidino-2-phenylindole (DAPI), the cationic steroid 3-[2(diethylamino)ethoxy]androst-5-en-17-one (U18666A), LysoTrackerRed (LTR), L-ascorbic acid, other chemicals and Superdex peptide were generated as described or obtained from sources listed previously (14, 24, 26, 27).

*Transfection*- pCEP4-APP encodes the APP695 cDNA cloned into NheI-XhoI cleaved pCEP4 (Invitrogen). Transfection was performed using Invitrogen's standard protocol for transfection with Lipofectamine 2000.

*Deconvolution Immunofluorescence Microscopy*- Cells were examined by immunofluorescence microscopy as described previously (24). In brief, cells were fixed in acetone in order to retain cellular and subcellular structure and to ensure the preservation of carbohydrates. The fixed cells were first pre-coated with 10% antimouse total Ig and then exposed to primary antibodies over night. The secondary antibodies used were Texas Red tagged goat anti-mouse Ig when the primary antibody was a monoclonal and FITC tagged goat anti-rabbit IgG or sometimes with FITC-tagged donkey anti-goat IgG when the primary antibody was a polyclonal. In the controls, the primary antibody was omitted. DNA staining with 4,6-diamidino-2-phenylindole (DAPI), as well as staining with antibodies was performed as recommended by the manufacturers. The fluorescent images were analyzed by using a Carl Zeiss AxioObserver inverted fluorescence microscope with deconvolution technique and equipped with objective EC "Plan-Neofluar" 63x/1.25 Oil M27 and AxioCam MRm Rev Camera. Identical exposure settings and times were used for all images. Several cells were observed before a representative image was selected. Images were also taken using the Z-stacking function in the AxioVision Rel. 4.8 software. Once the cell of interest was identified, a series of 10 images were automatically captured every 1.5 μm of the focal plane. Following capture the 10 images were combined into a movie to allow visualization of a 3-D image of the entire cell. In colocalization and quantification measurements using line-scan analysis, the fluorophores were excited in a sequential manner using Multi Track acquisition. This procedure minimizes channel cross-talk. Data analysis for colocalization was performed using Zeiss AxioVision Rel. 4.8 software.

*Confocal immunofluorescence microscopy*- Cells were analyzed by using a Zeiss LSM 710 confocal scanning equipment with a C-apochromat 63x/1.20 Water correction ring objective and Zen 2009 software. Colocalization analysis was performed with ImageJ 1.48v - module FIJI.

*Preparation of Nuclear Extract*- For preparation of the nuclear fraction, $5 \times 10^6$ in MEM containing 1 mM ascorbate and supplemented with 0.5% (w/v) BSA and 20 mM HEPES, pH 7.4, were treated with 6 mIU/ml heparinase I and 2 mIU/ml heparinase III for 30 min at 37$^{o}$C. Enzyme addition was repeated for another 30 min. Cells were washed off the plate, harvested by centrifugation and lysed. Intact nuclei were separated from "non-nuclear" cell components (cytosol, other organelles, and membrane fragments) using the standard protocol provided by the manufacturer (BioVision Research Products, Mountain View, CA). The purity of the preparation was assessed at each step by phase-contrast microscopy. The final preparation had no observable intact cells and consisted of bare nuclei. The nuclear preparation was lysed in 4 M guanidium chloride, 50 mM sodium acetate, pH 5.8.

*Radiolabeling and Identification of HS*- Labeling of cells with [$^{35}$S]sulfate and identification of radiolabeled HS by degradation with $HNO_2$ at pH 1.5 followed by gel exclusion chromatography on Superdex peptide was performed as described earlier (11, 28)

## RESULTS

*Formation and Nuclear Targeting of anMan-Containing HS Degradation Products is Dependent on APP/APLP2 Expression in Mouse Embryonic Fibroblasts (MEF)*- We have previously shown that proliferating human fetal lung fibroblasts constitutively generate Gpc-1-derived, anMan-containing HS degradation products, which was demonstrated by confocal immunofluorescence microscopy using an anMan-specific monoclonal antibody (mAb AM). However, as cells grow to confluence the anMan staining diminishes. Ascorbate can be taken up by growth-quiescent fibroblasts and induce deaminative autodegradation of Gpc-1 HS resulting in reappearance of anMan staining (14, 15).

We therefore examined by deconvolution immunofluorescence microscopy the appearance of anMan staining in near confluent cultures of mouse wild-type (Wt) MEF exposed to 1 mM ascorbate for different periods of time. In untreated cells and in cells treated for 1 min staining with mAb AM was undetectable (Fig. 1*A* and 1*B*, AM). After 5 min of ascorbate treatment anMan staining was visible in cytoplasmic vesicles (Fig. 1*C*, AM and DAPI). After 15 min, most of staining was in the nuclei (Fig. 1*D*) and after 1 h nuclear accumulation appeared to have reached its maximum (Fig. 1*E* and 1*F*). To confirm the nuclear localization we generated an image from a section through the center of a nucleus (Fig. 1*G*) and also a 3-D image of the nuclei (Fig. 1*H*).

To examine if expression of APP or APLP2 is required for formation and nuclear translocation of anMan-containing HS degradation products we investigated APP$^{-/-}$ and APLP2$^{-/-}$ MEF. While all Wt MEF observed showed nuclear anMan staining after ascorbate treatment (Fig. 2*A-B*, AM), very little anMan staining appeared in APP$^{-/-}$ and APLP2$^{-/-}$ MEF (Fig. 2*C-D* and Fig. 2*E-F*, AM). Tg2576 transgenic mice carry a mutation in APP that affects its processing and MEF from such mice overexpress APP and generate increased amounts of Aβ peptides. Treatment with ascorbate resulted in intense nuclear staining with mAb AM in all cells observed indicating that anMan-containing HS degradation products were produced in large amounts and accumulating in the nuclei of Tg2576 MEF (Fig. 2*G-H*, AM and DAPI).

In an attempt to restore formation and nuclear translocation of anMan-containing HS degradation products in $APP^{-/-}$ MEF, cells were transiently transfected with a vector encoding APP695 cDNA, treated with ascorbate and stained with mAb AM and a polyclonal antibody (pAb) to the C-terminal of APP (A8717). Transfected cells expressed APP (Fig. 2*J*, A8717, *cf.* Fig. 2*I*) and anMan staining of the nuclei was intense in these cells, indicating that APP expression is required for both formation and nuclear targeting of anMan-containing HS degradation products (Fig. 2*J*, AM and DAPI, *cf.* Fig. 2*I*).

To confirm that HS was present in the nuclei of Wt MEF upon ascorbate treatment, [$^{35}$S]sulfate-labeled cells were treated with ascorbate and a nuclear fraction was analyzed by gel exclusion chromatography on Superdex peptide before and after deaminative cleavage by nitrous acid at the HS-specific N-sulfated glucosamines. The amount of $^{35}$S-labeled glycosaminoglycans, eluting near the void volume, increased almost 3-fold after ascorbate treatment (Fig. 2*K-L*). In untreated cells, there was very little nuclear HS as judged from the relative insensitivity to nitrous acid (Fig. 2*K*, inset), whereas a large part of the nuclear glycosaminoglycans in ascorbate-treated cells consisted of HS (Fig. 2*L*, inset). Hence, the increase in nuclear $^{35}$S-labeled glycosaminoglycans can be attributed to accumulation of HS.

*Nuclear Targeting of anMan-Containing HS Degradation Products is Suppressed by β-Secretase Inhibition in Wt and Tg2576 MEF and by γ-Secretase Inhibition in Wt but not in Tg2576 MEF-* Both APP and APLP2 are processed by the β- and γ-secretases (1, 29). To determine if processing is required for endosome exit and nuclear import of the anMan-containing HS degradation products, we used the β- and γ-secretase inhibitors LY2811376 and BMS-708163, respectively. When Wt MEF were incubated with 100 nM LY2811376 for 48 h and then treated with 1 mM ascorbate for 1 h, the staining for anMan remained essentially extranuclear and nuclear accumulation of HS was prevented (Fig. 3*A-B*; *cf.* Fig. 2*A-B*). Treatment with 10 nM BMS-708163 partly suppressed nuclear import (Fig. 3*C-D*; *cf.* Fig. 2*A-B*). When Tg2576 MEF was incubated with the β-secretase inhibitor followed by ascorbate, nuclear anMan-staining was undetectable (Fig. 3*E-F*; *cf.* Fig. 2*G-H*). In contrast, treatment with 10 nM γ-secretase inhibitor was essentially unable to prevent ascorbate-induced nuclear import of anMan-containing HS-degradation products in Tg2576 MEF (Fig. 3*G-H*; *cf*. Fig. 2*G-H*). We also tested higher concentrations of the γ-inhibitor but the cells did not survive. Overall, β-secretase inhibition was considerably more effective than γ-secretase inhibition in blocking nuclear translocation of HS.

*Nuclear Targeting of anMan-Containing HS Degradation Products is Suppressed by β- and γ-Secretase Inhibition in N2a Neuroblastoma Cells*- APP and Gpc-1 colocalize in N2a neuroblastoma cells (10). These cells constitutively produce anMan-containing HS degradation products which are mainly located extranuclearly (15). To increase formation of these products by ascorbate treatment, endosomal accumulation of the Gpc-1-SNO precursor is required. This is achieved by pre-treatment with the synthetic cationic steroid 3-[2(diethylamino)ethoxy]androst-5-en-17-one (U18666A), which inhibits transport from early to late endosomes and thereby precludes deaminative cleavage of HS (15).

When N2a cells were treated with ascorbate only, anMan staining of the nuclei was negligible (Fig. 4*A*). However, treatment with U18666A followed by ascorbate resulted in intense nuclear staining by the anMan-specific mAb in most cells (Fig. 4*B*). To determine if APP processing by β- and/or γ-secretase was required for nuclear translocation of anMan-containing HS, N2a cells were treated with the respective inhibitors. In the presence of either LY2811376 or BMS-708163, anMan staining remained extranuclear in most cells following exposure to U18666A and ascorbate (Fig. 4*C-F*).

*Nuclear anMan-Containing HS Degradation Products are Exported to Autophagosomes*- Ishihara et al. (20) showed that a minor portion of HS derived from both endogenously produced and exogenously supplied [$^{35}$S] sulfate-labeled HS-proteoglycan accumulated, for up to 20 h, in the nuclei of rat hepatocytes and subsequently disappeared from the nuclei with a half-life of 8 h. We therefore examined whether the nuclear anMan-containing HS degradation products disappeared from the nuclei of wild-type MEF cells during chase in ascorbate-free medium. After 8 h of chase, the vast majority of the anMan-containing HS still remained in the nuclei; only a very weak, diffuse anMan staining was seen in the cytoplasm (Fig. 5*A*, left panels). However, after 24 h of chase, most the anMan-staining had disappeared from the nuclei and appeared to be both diffusely distributed in the cytosol and concentrated in cytoplasmic vesicles (Fig. 5*A*, middle panels). After 32 h of chase, the anMan-staining was exclusively associated with vesicles of varying size (Fig. 5*A*, right panels). To determine if the anMan-staining was associated with acidic vesicles, cells were also exposed to LysoTrackerRed (LTR) and examined by confocal microscopy. There was extensive (approx. 83%) colocalization between anMan-staining and LTR (Fig. 5*B*,) suggesting a phagosomal or lysosomal localization. Staining with anti-LC3, a recognized marker for autophagosomes (30), and also revealed extensive (approx. 87%) co-localization with the anMan-stained HS degradation products at paranuclear sites (Fig. 5*C*).

*anMan-Containing HS Degradation Products are Degraded in Lysosomes*- Nuclear recycling of HS may depend on the growth state of the cells. We therefore examined the location of anMan-containing HS degradation products in proliferating wild-type MEF by confocal microscopy. Most (approx. 87%) of the anMan-staining in ascorbate-treated proliferating cells appeared to be in acidic cytoplasmic vesicles (Fig. 6*A*,), suggesting a rapid transfer from endosomes into the nucleus and out to autophagosomes/lysosomes. Degradation in lysosomes can be impeded by treatment with chloroquine, a lysosomotropic agent that interferes with phagosome-lysosome fusion and/or lysosomal degradation (20). Accordingly, chloroquine treatment resulted in increased anMan staining that colocalized both with the nuclei (approx. 54%) and LTR-positive cytoplasmic vesicles (approx. 87%) (Fig. 6*B*). Thus, in proliferating MEF, the endosomal and nuclear HS pools may be small and most of the anMan-containing HS is undergoing degradation in lysosomes.

**DISCUSSION**

In addition to HS, a number of exogenous growth factors and their receptors can be targeted to the nucleus (23). Endocytosis of cell-surface proteins and HSPGs is well understood, but how they cross the lipid bilayer and escape into the cytosol remains an unresolved issue. HS, which is a highly polyanionic polysaccharide, is nevertheless transported from endosomes to the cytosol and then into the nucleus. We demonstrate that expression of APP and/or APLP2 is required to initiate an intracellular HS recycling route. anMan-Containing HS degradation products that are derived from Gpc-1 by constitutive or ascorbate-induced, SNO-dependent deaminative cleavage are transfered from endosomes into the cytosol and then into the nucleus. Eventually this HS disappears from the nucleus and is taken up by autophagosomes and degraded (Fig. 6*C* shows a schematic summary). We favor a non-vesicular transfer of HS through the cytosol since the anMan staining was diffuse both in the cytosol and in the nucleus. The present results also indicate that the traffic of anMan-containing HS is different between proliferating and growth-quiescent Wt MEF. In proliferating cells, anMan-containing HS is rapidly transfered to the nucleus and then to autophagosomes. In growth-quiescent MEF, the HS that is susceptible to deaminative cleavage is mainly attached to endosomal Gpc-1.

In previous studies (24) we did not observe extensive nuclear accumulation of anMan-containing HS when Tg2576 MEF was exposed to ascorbate for 3 h or more. The present results show that nuclear accumulation of HS is complete within 30 min in Wt MEF. Prolonged ascorbate treatment of Tg2576 MEF may have exhausted the Gpc-1-SNO pool and most of the HS may have reached the autophagosome compartment. Staining with mAb AM could be affected by changes in HS structure and/or by epitope availability. Changes in HS structure near the anMan of the reducing end after release from Gpc-1 by heparanase cleavage is unlikely as its cleavage sites should be far removed from the reducing end. In the nucleus where HS can interact strongly with the basic histones, epitope availability did not appear to be a problem.

Nuclear translocation of anMan-containing HS was affected by inhibition of β- and γ-secretases. Although the inhibitors used could affect other signaling pathways, it appears likely that APP/APLP2 degradation products are involved in the endosome-to-cytosol transfer. The β-inhibitor efficiently blocked nuclear uptake in both Wt and Tg2576 MEF as well as in N2a cells. β-Cleavage generates a soluble N-terminal APP fragment (sAPPβ) and a membrane-bound C-terminal one (βCTF) which may be involved in the S-nitrosylation of Gpc-1 (10) and in the transfer of HS across the lipid bilayer, respectively. The γ-inhibitor efficiently blocked nuclear targeting in N2a cells, while it was less efficient in Wt MEF and totally inactive in Tg2576 MEF. These results imply that Aβ peptides and/or Aβ-like peptides as well as the remaining C-terminal fragment of APP (γCTF) may also be involved. The lack of effect in Tg2576 MEF may reflect an inability to reach a sufficiently high inhibitor concentration to diminish production of Aβ.

Aβ peptides can assume a variety of oligomeric conformations some of which may be pore-forming or may function as cell-penetrating peptides that can deliver large-cargo molecules, including HS, into cells (2, 31-33). Such Aβ assemblies, formed *in vitro*, can be toxic to cells (2). However, we have recently shown that Aβ assemblies formed in the presence of anMan-containing HS degradation products are non-toxic (25). It is possible that complexes between Aβ peptides and anMan-containing HS are involved in endosomal exit of HS. Thereby, formation of toxic Aβ is precluded.

The deaminative cleavage sites in Gpc-1 HS are preferentially located near the linkage region to the core protein. Therefore, the anMan-containing HS degradation products consist mostly of almost full-length HS chains (11, 29). The nuclear HS isolated from hepatocytes was also of polysaccharide size (19).

The functional role of HS inside the nucleus remains to be elucidated. Earlier studies have implicated histones, transcription factors, kinases and topoisomerases as target molecules (34). Evidence that nuclear HS regulates the cell cycle, proliferation, transcription and nuclear import of cargo is mounting (35).

Nuclear import of anMan-containing HS may require binding to proteins that contain a nuclear localization signal (35). The anMan residue, which contains a free aldehyde, can couple reversibly to amino groups in proteins via an aldimine bond. HS may transport positively charged cargo from the cytosol into the nucleus (31) and/or serve as a scavenger of misfolded nuclear proteins and transport them to autophagosomes for destruction. This should be particularly important for non-dividing cells, like neurons. Manipulations of Aβ production may thus have deleterious effects upon HS function in the nucleus. The present findings may also contribute to an understanding of the physiological function of APP which is still incomplete (36).

**REFERENCES**


1. Walsh, D.M., Minogue, A.M., Sala Frigerio, C., Fadeeva, J.V., Wasco, W. and Selkoe, D.J. (2007) The APP family of proteins: similarities and differences. *Biochem. Soc. Trans.* **35**, 416-420
2. Benilova, I., Karran, E. and De Strooper, B. (2012) The toxic Aβ oligomer and Alzheimer´s disease: an emperor in need of clothes. *Nature Neurosci.* **15**, 1-9
3. Gouras, G.K., Willén, K. and Tampellini, D. (2012) Critical role of intraneuronal Aβ in Alzheimer´s disease: Technical challenges in studying intracellular Aβ. *Life Sci.* **91**, 1153-1158
4. Larson, M.E. and Lesné, S.E. (2012) Soluble Aβ oligomer production and toxicity. *J. Neurochem.* **120**, 125-139
5. Müller, U.C. and Zheng, H. (2012) Physiological functions of APP family proteins. *Cold Spring Harb. Perspect. Med.* **4,** a006288
6. Abramov, E., Dolev, I., Fogel, H., Ciccotosto, G.D., Ruff, E. and Slutsky, I. (2009) Amyloid-β as a positive endogenous regulator of release probability at hippocampal synapses. *Nature Neurosci.* **12**, 1567-1576

7. Reinhard, C., Hébert, S.S. and De Strooper, B. (2005) The amyloid-β precursor protein: integrating structure with biological function. *EMBO J.* **24**, 3996-4006
8. Williamson, T.G., Mok, S.S., Henry, A., Cappai, R., Lander, A.D., Nurcombe, V., Beyreuther, K., Masters, C.L. and Small, D.H.. (1996) Secreted glypican binds to the amyloid precursor protein of Alzheimer´s disease (APP) and inhibits APP-induced neurite outgrowth. *J. Biol. Chem.* **271,** 31215-31221
9. Watanabe, N., Araki, W., Chui, D.H., Makifuchi, T., Ihara, Y. and Tabira, T. (2004) Glypican-1 as an Abeta binding HSPG in the human brain: its localization in DIG domains and possible roles in the pathogenesis of Alzheimer´s disease. *FASEB J.* **18,** 1013-1015
10. Cappai, R, Cheng, F., Ciccotosto, G.D., Needham, B.E., Masters, C.L., Multhaup, G., Fransson, L.-Å. and Mani, K. (2005) The amyloid precursor protein (APP) of Alzheimer disease and its paralog, APLP2, modulate the Cu/Zn-nitric oxide-catalyzed degradation of glypican-1 heparan sulfate in vivo. *J. Biol. Chem.* **280**, 13913-13920
11. Ding, K., Mani, K., Cheng, F., Belting, M. and Fransson, L.-Å. (2002) Copper-dependent autocleavage of glypican-1 heparan sulfate by nitric oxide derived from intrinsic nitrosothiols. *J. Biol. Chem.* **277,** 33353-33360
12. Cheng, F., Mani, K., van den Born, J., Ding, K., Belting, M. and Franssson, L.-Å. (2002) Nitric oxide-dependent processing of heparan sulfate in recycling S-nitrosylated glypican-1 takes place in caveolin-1 containing endosomes. *J. Biol. Chem.* **277,** 44431-44439
13. Mani, K., Cheng, F., Havsmark, B., Jönsson, M., Belting, M. and Fransson, L.-Å. (2003) Prion,amyloid-β-derived Cu(II) ions or free Zn(II) ions support S-nitroso-dependent autocleavage of glypican-1 heparan sulfate. *J. Biol. Chem.* **278,** 38956-38965
14. Mani, K., Cheng, F. and Fransson, L.-Å. (2006) Defective NO-dependent, deaminative cleavage of glypican-1 heparan sulfate in Niemann-Pick C1 fibroblasts. *Glycobiology* **16,** 711-718
15. Mani, K., Cheng, F. and Fransson, L.-Å. (2006) Constitutive and vitamin C-induced, NO-catalyzed release of heparan sulfate from recycling glypican-1 in late endosomes. *Glycobiology* **16,** 1251-1261
16. Svensson, G. and Mani, K. (2009) S-nitrosylation of secreted recombinant human glypican-1. *Glycoconjugate J.* **26,** 1247-1257
17. Cheng, F., Svensson, G., Fransson, L.-Å. and Mani, K. (2012) Non-conserved, S-nitrosylated cysteines in glypican-1 react with N-unsubstituted glucosamines in heparan sulfate and catalyze deaminative cleavage. *Glycobiology* **22**, 1480-1486
18. Bhavanandan, V.P. and Davidson, E.A. (1975) Mucopolysaccharides associated with nuclei of cultured mammalian cells. *Proc. Natl. Acad. Sci. U.S.A.* **72**, 2032-2036

19. Fedarko, N.S. and Conrad, H.E. (1986) A unique heparan sulfate in the nuclei of hepatocytes. Structural changes with the growth state of the cells. *J. Cell Biol.* **102**, 587-599
20. Ishihara, M., Fedarko, N.S. and Conrad, H.E. (1986) Transport of heparan sulfate into the nuclei of hepatocytes. *J. Biol. Chem.* **261**, 13575-13580
21. Hiscock, D.R.R., Yanagishita, M. and Hascall, V.C. (1994) Nuclear localization of glycosaminoglycans in rat ovarian granulosa cells. *J. Biol. Chem.* **269,** 4539-4546
22. Mani, K., Belting, M., Ellervik, U., Falk, N., Svensson, G., Sandgren, S., Cheng, F. and Fransson, L.-Å. (2004) Tumor attenuation by 2(6-hydroxynaphthyl)-β-D-xylopyranoside requires priming of heparan sulfate and nuclear targeting of the product. *Glycobiology* **14**, 387-397
23. Bryant, D.M. and Stow, J.L. (2005) Nuclear translocation of cell-surface receptors: lessons from fibroblast growth factor. *Traffic* **6**, 947-954
24. Cheng, F., Cappai, R., Ciccotosto, G.D., Svensson, G., Multhaup, G., Fransson, L.-Å. and Mani, K. (2011) Suppression of amyloid β A11 antibody immunoreactivity by vitamin C. Possible role of heparan sulfate oligosaccharides derived from glypican-1 by ascorbate-induced, nitric oxide (NO)-catalyzed degradation. *J. Biol. Chem.* **286**, 27559-27572
25. Cheng, F., Ruscher, K., Fransson, L.-Å. and Mani, K. (2013) Non-toxic amyloid beta formed in the presence of glypican-1 or its deaminatively generated heparan sulfate degradation products. *Glycobiology* **23**, 1510-1519
26. Belting, M., Mani, K., Jönsson, M., Cheng, F., Sandgren, S., Jonsson, S., Ding, K., Delcros, J.-G. and Fransson, L.-Å. (2003) Glypican-1 is a vehicle for polyamine uptake in mammalian cells. A pivotal role for nitrosothiol-derived nitric oxide. *J. Biol. Chem.*, **278**, 47181-47189
27. Mani, K., Cheng, F. and Fransson, L.-Å. (2007) Heparan sulfate degradation products can associate with oxidized proteins and proteasomes. *J. Biol. Chem.* **282,** 21934-21944
28. Ding, K., Sandgren, S., Mani, K., Belting, M. and Fransson, L.-Å. (2001) Modulations of glypican-1 heparan sulfate structure by inhibition of endogenous polyamine synthesis. Mapping of spermine-binding sites and heparanase, heparin lyase and nitric oxide/nitrite cleavage sites. *J. Biol. Chem.* **276**, 46779-46791
29. Hogl, S., Kuhn, P.-H., Colombo, A. and Lichtenthaler, S.F. (2011) Determination of the proteolytic cleavage sites of the amyloid precursor-like protein 2 by the proteases ADAM10, BACE1 and γ-secretase. *PLoS ONE* **6,** e21337
30. Nixon, R.A. (2013) The role of autophagy in neurodegenerative disease. *Nature Med.* **19**, 983-997
31. Sandgren, S., Wittrup, A., Cheng, F., Jönsson, M., Eklund, E., Busch, S. and Belting, M. (2004) The human antimicrobial peptide LL-37 transfers extracellular DNA plasmids to the nuclear

compartment of mammalian cells via lipid rafts and proteoglycan-dependent endocytosis. *J. Biol. Chem.* **279**, 17951-17956

32. Kagan, B.L. (2012) Membrane pores in the pathogenesis of neurodegenerative disease. *Proc. Mol. Biol. Transl. Sci.* **107**, 295-325
33. Regberg, J., Eriksson, J.N. and Langel, U. (2013) Cell-penetrating peptides: from cell cultures to in vivo applications. *Front. Biosci.* **5E**, 509-516
34. Dudas, J., Ramadori, G., Knittel, T., Neubauer, K., Raddatz, D, Egedy, K., and Kovalsky, I. (2000) Effect of heparin and liver heparan sulphate on interaction of HepG2-derived transcription factors and their *cis*-acting elements: altered potential of hepatocellular carcinoma heparan sulphate. *Biochem. J.* **350**, 245-251
35. Stewart, M.D. and Sanderson, R.D. (2013) Heparan sulfate in the nucleus and its control of cellular functions. *Matrix Biol.* http://dx.**doi.**org/10.1016/j.matbio.2013.10.009
36. Shariati, S.A.M. and De Strooper, B. (2013) Redundancy and divergence in the amyloid precursor protein family. *FEBS Letters* **587,** 2036-2045

**FOOTNOTES**

***** This work was supported by grants from the Swedish Research Council, Alfred Österlund, Kock, and Olle Engkvist Foundations to F.C., L.-Å.F. and K.M., the National Health and Medical Research Council (NHMRC) of Australia to R.C., and the Swedish Cancer Society to M.B.

[3] To whom correspondence should be addressed. E-mail: katrin.mani@med.lu.se

[4] The abbreviations used are: Aβ, amyloid beta; AD, Alzheimer´s disease; anMan/AM, anhydromannose; APLP1/2, amyloid precursor like protein1/2; APP, amyloid precursor protein; DAPI, 4,6-diamidino-2-phenylindole; Gpc-1, glypican-1; HS, heparan sulfate; LTR, LysoTrackerRed; mAb, monoclonal antibody; MEF, mouse embryonic fibroblast; pAb, polyclonal antibody; SNO, S-nitrosothiol; Tg2576, Transgenic AD mouse; U18666A, 3-[2(diethylamino)ethoxy]androst-5-en-17-one.

**LEGENDS TO THE FIGURES**

FIGURE 1. **Time-course of nuclear accumulation of anMan-containing HS degradation products in ascorbate-treated mouse embryonic fibroblasts (MEF).** Representative immunofluorescence images of wild-type (Wt) MEF cells exposed to 1 mM ascorbate for the indicated periods of time (*A*-*F*). (*G*) A horizontal section at 7.77 μm from the top of a nucleus. (*H*) 3-D image of the cell nuclei. This experiment has been repeated 5 times. AM, anhydromannose; DAPI, nuclear stain.

FIGURE 2. **Formation and nuclear targeting of anMan-containing HS degradation products is dependent on APP/APLP2 expression in mouse embryonic fibroblasts (MEF).** Representative immunofluorescence images of (*A*-*B*) wild-type (Wt) MEF cells, (*C*-*D*) $APP^{-/-}$ cells, (*E*-*F*) $APLP2^{-/-}$ cells, (*G*-*H*) Tg2576 cells and (*I*-*J*) APP-/- cells (*I*) untransfected or (*J*) transfected with a vector encoding APP. Cells were untreated or treated with 1 mM ascorbate for 1 h and stained with DAPI and mAb AM. Bar, 20 μm. Exposure times were the same in all cases. Tg2576, MEF from AD mouse model; AM, anhydromannose; DAPI, nuclear stain; A8717, antibody to C-terminus of APP; Asc, ascorbate. (*K*-*L*) Wt MEF (T-25 dishes) were grown to confluence in $^{35}$S-sulfate containing medium, treated with HS lyase to remove pericellular HS, washed and extracted sequentially with detergents (see Materials and methods) to obtain a nuclear fraction, which was lysed and chromatographed on a column of Superdex peptide in 4 M guanidinium chloride. The nuclear extracts were obtained from cells that were (*K*) untreated or (*L*) treated with 1 mM ascorbate for 1 h. The void volume ($V_o$) fractions were pooled (see bars in K and L), recovered by ethanol precipitation in the presence of HS carrier, treated with $HNO_2$ at pH 1.5 and re-chromatographed (insets in *K*-*L*). Identical aliquots of the fractions were analyzed for radioactivity by β-scintillation. Di, disaccharide elution position; $^{35}SO_4$, sulfate elution position; $V_t$, total volume. These experiments have been performed twice.

FIGURE 3. **Nuclear targeting of anMan-containing HS degradation products is suppressed by β-secretase inhibition in Wt and Tg2576 MEF and by γ-secretase inhibition in Wt but not in Tg2576 MEF.** Representative immunofluorescence images of (*A*-*D*) wild-type MEF cells and (*E*-*H*) Tg2576 cells treated with (*A*,*B*,*E*,*F*) 100 nM β-inhibitor or (*C*,*D*,*G*,*H*) 10 nM γ-inhibitor both for 48 h followed by (*B*,*D*,*F*,*H*) treatment with 1 mM ascorbate for 1 h and then stained with DAPI and mAb AM. Bar, 20 μm. Tg2576, MEF from AD mouse model; AM, anhydromannose; DAPI, nuclear stain; Asc, ascorbate. These experiments have been repeated twice.

FIGURE 4. **Nuclear targeting of anMan-containing HS degradation products is suppressed by β- and γ-secretase inhibition in N2a neuroblastoma cells**. Representative immunofluorescence images of cells treated with (*A*) 1 mM ascorbate for 1 h, with (*C*, *E*) 100 nM β-inhibitor or (*D*, *F*) 10 nM γ-inhibitor both for 48 h, with (*B*-*F*) 3 μg/ml U18666A from t=32 h to t=48 h followed by (*B*, *E*, *F*) 1 mM ascorbate for 1 and then stained with DAPI and mAb AM. Merged, DAPI/AM. Bar, 20 μm. N2a, neuroblastoma cells; AM, anhydromannose; DAPI, nuclear stain; Asc, ascorbate; U18, U18666A, inhibitor of endosomal traffic. These experiments have been repeated twice.

FIGURE 5. **Nuclear anMan-containing HS degradation products are exported to autophagosomes**. Representative immunofluorescence images of Wt MEF treated with 1 mM ascorbate for 1 h, then chased in fresh medium for various periods of time (t=4, 6, 8, 24 and 32 h). Staining was performed with (*A*) DAPI and mAb AM, (*B*) DAPI, mAb AM and LTR and (*C*) DAPI, mAb AM and pAb LC3. Deconvolution microscopy was performed in A and confocal microscopy in B and C. (*B*) Merged image of DAPI, AM and LTR; (*C*) merged image of DAPI, AM and LC3. Insets in B and C show scatter grams that estimates the extent of colocalization (Pearsons´s R value) for (*B*) AM and LTR and (*C*) AM and LC3. Bar, 20 μm. AM, anhydromannose; DAPI, nuclear stain; LTR, LysoTrackerRed; LC3, autophagosome marker. These experiments have been repeated three times.

FIGURE 6. **anMan-Containing HS degradation products are degraded in lysosomes.** Representative confocal immunofluorescence images of proliferating Wt MEF (*A*) treated with 1 mM ascorbate for 1 h or (*B*) 0.1 mM chloroquine overnight. Staining was performed with DAPI, mAb AM and LysoTrackerRed (LTR). Inset in A shows scatter gram that estimates the extent of colocalization (Pearson´s R value) for AM and LTR. Insets in B show corresponding scatter grams for (*I*) AM and LTR and (*II*) DAPI and AM. Bar, 20 μm. AM, anhydromannose; DAPI, nuclear stain; Asc, ascorbate; Chl, chloroquine. This experiment has been repeated twice. (*C*) Schematic summary of major findings in the present work; *1*, Gpc-1 is S-nitrosylated (SNO) in a copper-dependent reaction supported by APP; *2*, anMan-containing HS (HS-anMan) is released from Gpc-1 and transfered into the cytosol supported by APP/APLP2 and /or its degradation products; *3*, HS-anMan enters the nucleus; *4*, HS-anMan leaves the nucleus; *5*, HS-anMan is captured in autophagosomes and eventually degraded in lysosomes.

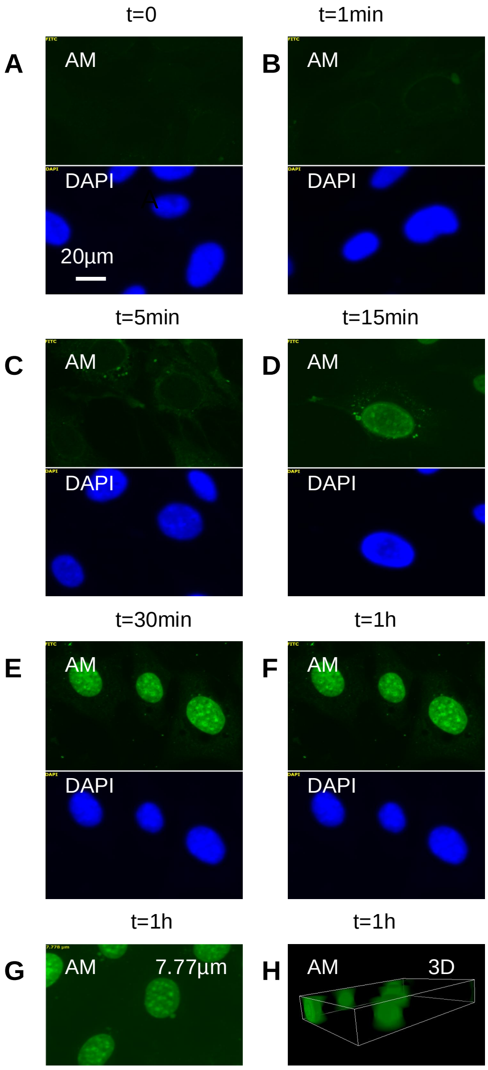
t=0
t=1min
A
AM
DAPI
20µm
B
AM
DAPI
t=5min
t=15min
C
AM
DAPI
D
AM
DAPI
t=30min
t=1h
E
AM
DAPI
F
AM
DAPI
t=1h
t=1h
G
AM
7.77µm
H
AM
3D

Fig.1

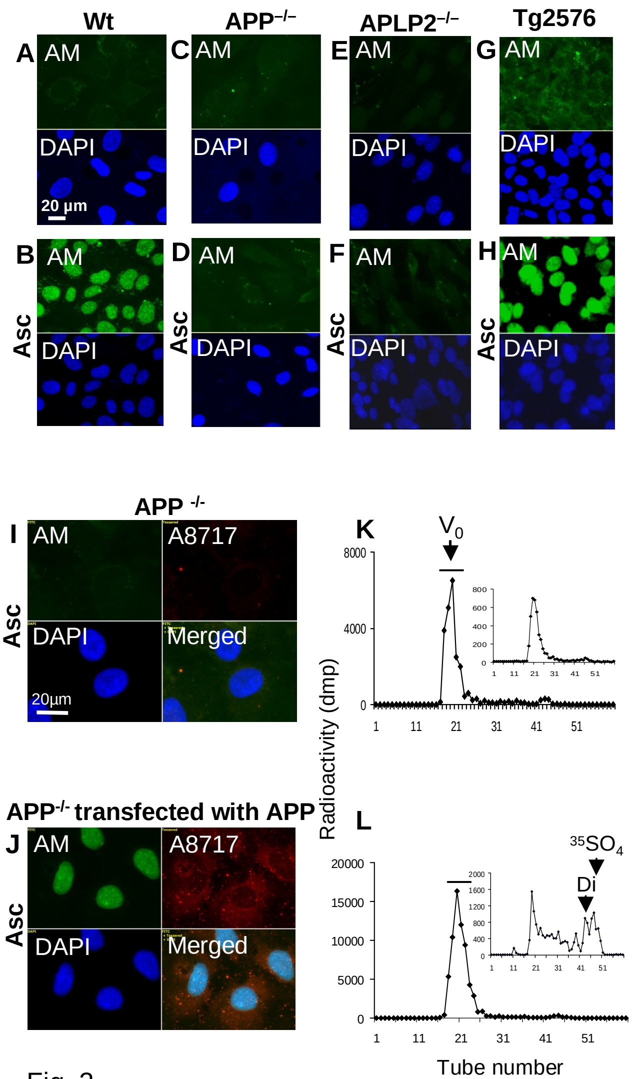

Wt
APP−/−
APLP2−/−
Tg2576
A
AM
DAPI
20 µm
C
AM
DAPI
E
AM
DAPI
G
AM
DAPI
B
AM
DAPI
Asc
D
AM
DAPI
Asc
F
AM
DAPI
Asc
H
AM
DAPI
Asc
APP -/-
I
AM
A8717
DAPI
Merged
20µm
Asc
K
V0
8000
4000
0
1
11
21
31
41
51
Radioactivity (dmp)
APP-/- transfected with APP
J
AM
A8717
DAPI
Merged
Asc
L
35SO4
Di
20000
15000
10000
5000
0
1
11
21
31
41
51
Tube number


Fig. 2

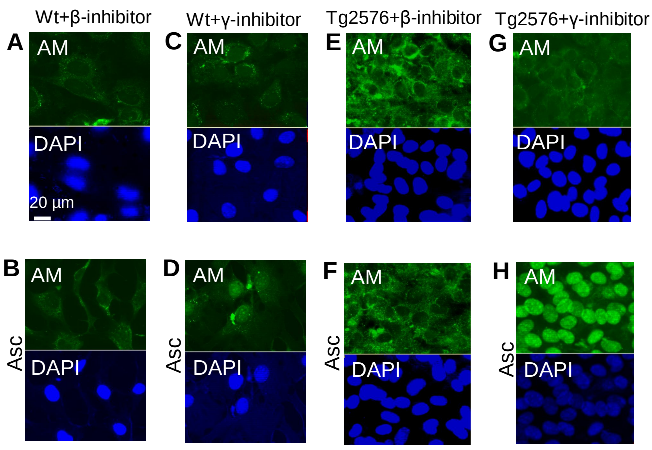
Wt+β-inhibitor
Wt+γ-inhibitor
Tg2576+β-inhibitor
Tg2576+γ-inhibitor
A
AM
DAPI
20 µm
C
AM
DAPI
E
AM
DAPI
G
AM
DAPI
B
AM
DAPI
Asc
D
AM
DAPI
Asc
F
AM
DAPI
Asc
H
AM
DAPI
Asc

Fig. 3

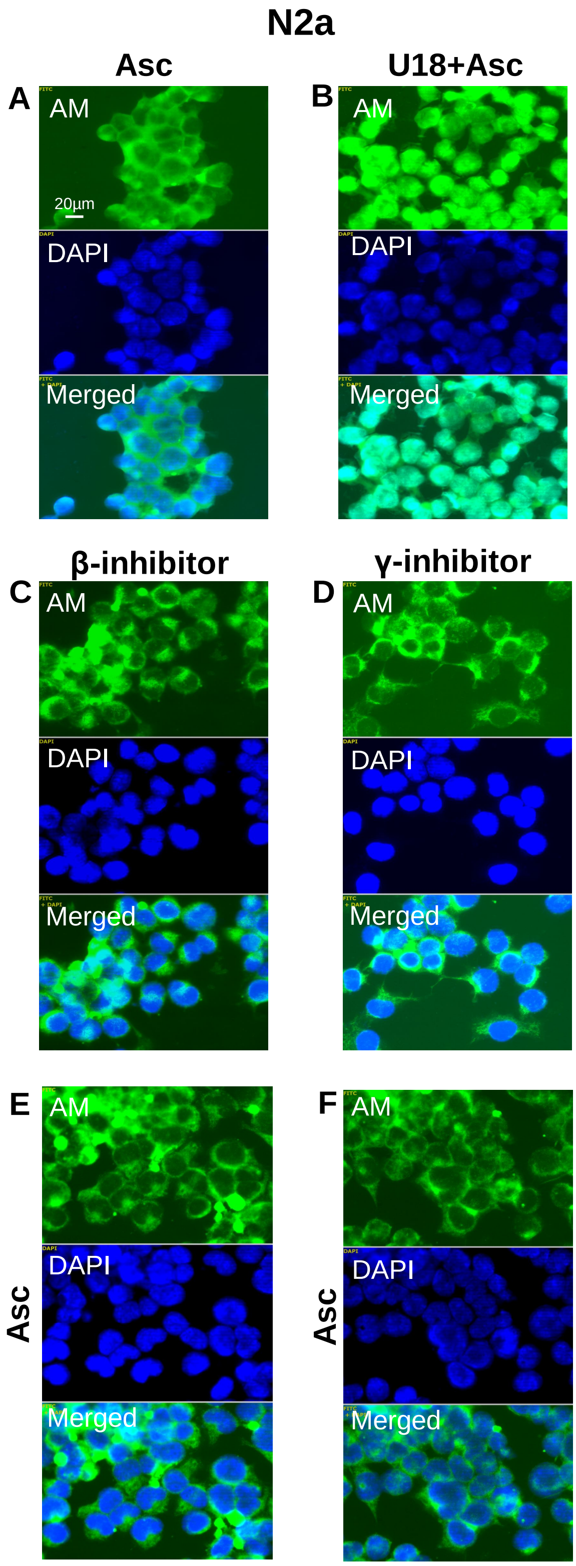
N2a
Asc
U18+Asc
A
AM
20μm
DAPI
Merged
B
AM
DAPI
Merged
β-inhibitor
γ-inhibitor
C
AM
DAPI
Merged
D
AM
DAPI
Merged
E
AM
DAPI
Merged
Asc
F
AM
DAPI
Merged
Asc

Fig. 4

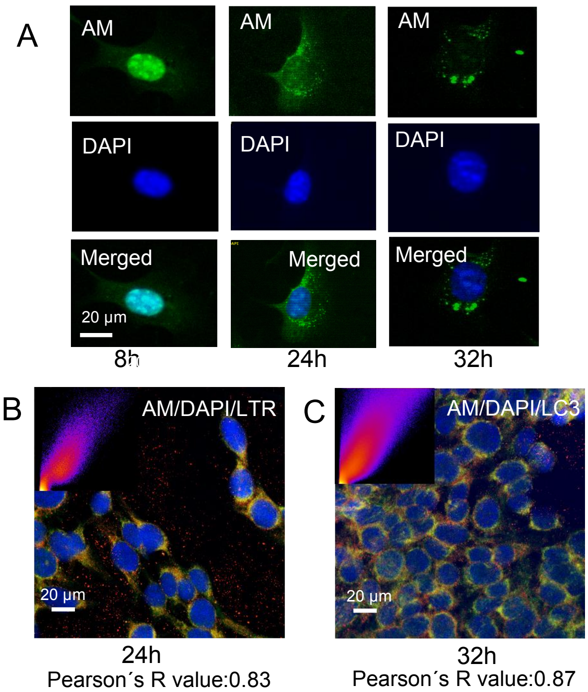
A
AM
AM
AM
DAPI
DAPI
DAPI
Merged
Merged
Merged
20 μm
8h
24h
32h
B
AM/DAPI/LTR
20 μm
C
AM/DAPI/LC3
20 μm
24h
Pearson´s R value:0.83
32h
Pearson´s R value:0.87

Fig.5

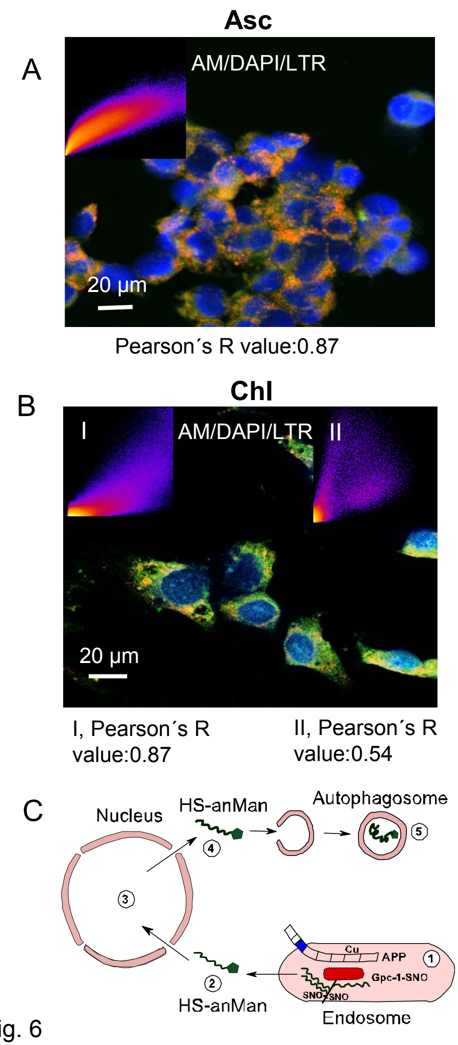
Asc
A
AM/DAPI/LTR
20 µm
Pearson´s R value:0.87
Chl
B
I
AM/DAPI/LTR
II
20 µm
I, Pearson´s R value:0.87
II, Pearson´s R value:0.54
C
Nucleus
HS-anMan
Autophagosome
4
5
3
Cu
APP
1
Gpc-1-SNO
SNO
SNO
2
HS-anMan
Endosome

Fig. 6